

# Metal-semiconductor Transition with Anomalous Thermal Hysteresis Observed in Hexagonal $(\text{Ni}_{1-x}\text{Fe}_x)_{1-y}\text{S}$ , $(0 \leq x \leq 0.30, 0 \leq y \leq 0.035)$

Tsukio OHTANI,\*† Koji KOSUGE, and Sukeji KACHI

Department of Chemistry, Faculty of Science, Kyoto University, Sakyo-ku, Kyoto 606

(Received July 7, 1980)

The phase relation of  $(\text{Ni}_{1-x}\text{Fe}_x)_{1-y}\text{S}$  system was determined by the X-ray powder diffraction method.  $\text{Fe}_{1-y}\text{S}$  can be dissolved in  $\text{Ni}_{1-y}\text{S}$  in *ca.* 30 at.%. Transition temperature ( $T_t$ ) was measured mainly by the DSC method.  $T_t$  increases with increase in Fe contents.  $T_t$  in the forward direction, however, shows a significant increase as high as 50 degrees, when specimens are aged at a temperature below  $T_t$ . The reverse transformation is not affected by thermal history at all. This is explained by the relaxation process in which the strain energy stored in the low temperature phase is relieved by aging.

NiS (NiAs structure) can be obtained by quenching from high temperature (above 600 K).<sup>1)</sup> The first detailed investigations of NiS were performed by Sparks and Komoto<sup>2–4)</sup> who found that NiS shows a first-order phase transition at  $T_t = 265$  K, the high temperature phase (H-phase) being a Pauli paramagnetic metal and the low temperature phase (L-phase) an antiferromagnetic semiconductor. They also found that the cell volume expands by *ca.* 2.0% through  $T_t$  with fall in temperature.<sup>3)</sup> Trahan *et al.* performed powder X-ray diffraction measurements and found a crystal symmetry change at  $T_t$ .<sup>5)</sup> On the other hand MacWhan *et al.* found no crystal symmetry change by X-ray study of single crystals.<sup>6)</sup> Various electrical measurements revealed that the H-phase is a normal metal with n-type conduction and the L-phase a p-type semiconductor.<sup>7–12)</sup> One of us (T. O.) found that the L-phase is a degenerate semiconductor in which carriers are substantially produced from Ni vacancies.<sup>9)</sup> On the basis of magnetic measurements, the H-phase is considered to be a weakly-correlated Pauli paramagnet and the L-phase an antiferromagnet with the itinerant nature.<sup>13,14)</sup>  $T_t$  is lowered by the deviation from stoichiometry<sup>4)</sup> and by external pressure.<sup>15,16)</sup>  $T_t$  is also sensitive to the impurity ions.<sup>17–20)</sup> Thermal hysteresis at  $T_t$  was reported by many authors. The hysteresis width is several degrees.<sup>9,21)</sup> Trahan and Goodrich, however, reported that an extremely long time is required for the equilibrium near the transition, the thermal hysteresis width being about ten degrees.<sup>22)</sup>

There are less complete data and discussions on the origin of the transition. It was found that the enthalpy change at  $T_t$  is about  $5.0 \text{ J mol}^{-1} \text{ deg}^{-1}$  for stoichiometric NiS.<sup>21,22)</sup> Some authors assumed that the large part of entropy change at the transition is due to lattice contribution, suggesting the importance of electron-lattice interaction.<sup>9,23)</sup> Strong electron-correlation effect would also play an important role in this transition, as in the case of some transition metal oxides such as  $\text{V}_2\text{O}_3$  and related vanadium oxides.<sup>24)</sup> White and Mott first discussed this transition on the basis of correlation effects.<sup>25)</sup> So far, we have few data on NiS which suggest the effect.

The pseudo-binary NiS–FeS system was investigated

by Misra and Fleet.<sup>26)</sup> They found that the solubility of  $\text{Fe}_{1-y}\text{S}$  into  $\text{Ni}_{1-y}\text{S}^{**}$  increases with increasing  $y$  (metal deficiency). Continuous solid solution of this system was found to be in metal-poor region above 500 °C.  $T_t$  of NiS, Ni being substituted by Fe, has been observed.<sup>17,19,20)</sup> We reported that  $T_t$  is raised by substitution of Fe ions ( $T_t$  increases by about 20 K for 2.0% of Fe substitution), suggesting that the increase in  $T_t$  is significantly related to the increase of cell volume.<sup>17)</sup> Recently Coey *et al.*<sup>23)</sup> and Barthelemy *et al.*<sup>19)</sup> investigated the system  $(\text{Ni}_{1-x}\text{Fe}_x)_{1-y}\text{S}$ . The former proposed the phase diagram in the region with  $x < 0.10, y \approx 0.04$ , which is classified into three distinct regions according to their magnetic behavior. The latter observed two phases: the region with  $0 \leq x \leq 0.05$  and that with  $0.10 \leq x \leq 0.20$  where c-parameter is greater than that in the first region. So far, no systematic investigation on this system seems to have been performed. No detailed report has appeared on the thermal hysteresis of this transition. We have investigated  $(\text{Ni}_{1-x}\text{Fe}_x)_{1-y}\text{S}$  solid solution and the effects of Fe substitution on the phase transition of NiS in the wide composition range and the anomalous thermal hysteresis of the transition.<sup>27)</sup> In this paper, we will report the results of investigations.

## Experimental

Starting samples of  $\text{Ni}_{1-y}\text{S}$  and  $\text{Fe}_{1-y}\text{S}$  were prepared separately from the pure elements. The method is the same as that reported.<sup>9)</sup>  $\text{Ni}_{1-y}\text{S}$  and  $\text{Fe}_{1-y}\text{S}$  obtained were mixed in an appropriate ratio and heated at 1000 °C in evacuated silica tubes for a week, and then quenched into cold water after being annealed at 800 °C for 3 d. Reground samples were heated at 1000 °C and then annealed at temperatures 150–800 °C for a month. Annealed samples were quenched into cold water. Several kinds of measurements were performed for powder and ingot specimens. X-Ray powder diffraction measurements were made on annealed samples. The temperature dependence of the lattice constants was measured in the temperature range 270–360 K for  $(\text{Ni}_{0.8}\text{Fe}_{0.2})_{0.965}\text{S}$ . DSC measurements were carried out with a Rigaku Thermoflex DSC at 110–373 K using  $\text{Al}_2\text{O}_3$  as a reference, measurements being made on polycrystals ground in an agate mortar. Aging effects on  $T_t$  were measured by the DSC method. Electrical resistivity measurements were performed by an ordinary four

† Present address: Okayama University of Science, Laboratory for Solid State Chemistry, 1-1 Ridaicho, Okayama 700.

\*\* Suffix, 1–y, means that nonstoichiometric specimens contain only the deficient metals.

probes method on ingot samples, and aging effects on resistivity were examined at 290 K. Magnetic susceptibility was measured with a Faraday type torsion balance from liquid  $\text{N}_2$  temperature to 373 K. Mössbauer effect measurements were carried out on  $(\text{Ni}_{0.8}\text{Fe}_{0.2})_{0.985}\text{S}$  with a conventional spectrometer in a transmission setting at liquid  $\text{N}_2$  temperature and at 373 K for samples of both immediately after quenching and after aging for 20 days.

## Results

**Phase Identification.** Phase determination of the pseudo-binary  $\text{Ni}_{1-y}\text{S}-\text{Fe}_{1-y}\text{S}$  system was made on the identification of X-ray powder pattern for quenched samples. Figure 1(a) shows the phase relation of  $\text{Ni}_{1-y}\text{S}-\text{Fe}_{1-y}\text{S}$  system at 800 °C. The closed square indicates hexagonal NiAs phase and the open square two-phase region consisting of NiAs phase and cubic pentlandite phase,  $(\text{Fe,Ni})_9\text{S}_8$ . Stoichiometric NiS takes only less than 30 at. % FeS into solid solution. A continuous solid solution was found to exist in the metal-poor region ( $y \leq 0.035$ ). No extra line due to

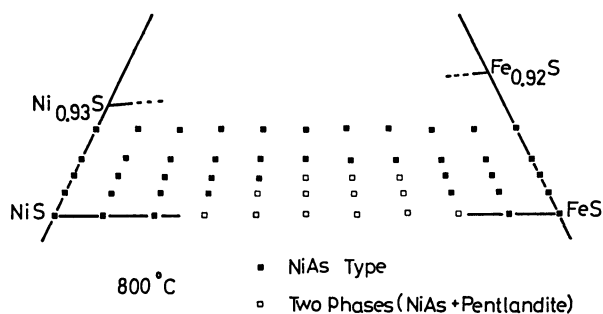


Fig. 1(a). Phase relations of pseudo-binary  $\text{Ni}_{1-y}\text{S}-\text{Fe}_{1-y}\text{S}$  system obtained by quenching from 800 °C. The closed square indicates the hexagonal solid solution (NiAs-type), and the open square the two phase region consisting of hexagonal NiAs and cubic pentlandite phase.

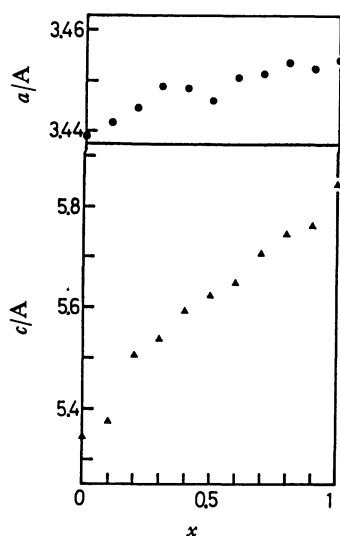


Fig. 1 (b). Lattice spacings measured at room temperature of  $(\text{Ni}_{1-x}\text{Fe}_x)_{0.985}\text{S}$  quenched from 800 °C. a-axis is shown by circles and c-axis triangles. Fe contents is taken as abscissa.

superstructure development as reported by Misra and Fleet was observed in all samples within experimental errors. At lower temperatures, the two phase region spreads out towards metal-poor compositions; for example at 150 °C the two phase region on NiS-FeS line extends from 20 to 80% of FeS concentration, while on a  $\text{Ni}_{0.955}\text{S}-\text{Fe}_{0.955}\text{S}$  line only up to 20% of  $\text{Fe}_{0.955}\text{S}$  can be dissolved into  $\text{Ni}_{0.955}\text{S}$ . Figure 1(b) shows the lattice spacings of the continuous solid solution of  $(\text{Ni,Fe})_{0.985}\text{S}$  at 800 °C. The a-parameter curve as a function of composition has a minimum at 50 at. % of Fe, while c-parameter changes smoothly with Fe contents.

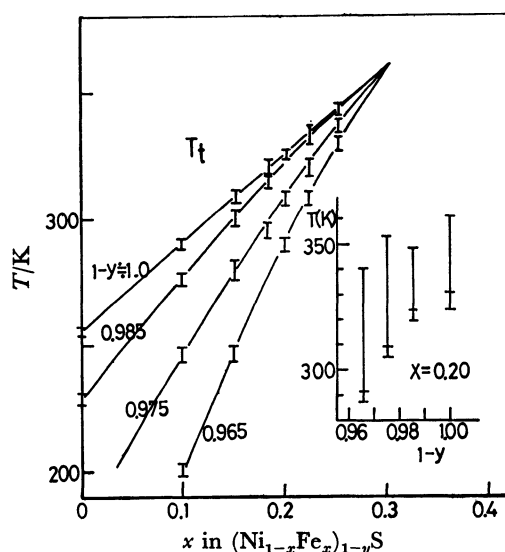


Fig. 2. Transition temperatures ( $T_t$ ) of  $(\text{Ni}_{1-x}\text{Fe}_x)_{1-y}\text{S}$  obtained by DSC measurements. Measurements were carried out on specimens immediately after quenching.  $x$  in  $(\text{Ni}_{1-x}\text{Fe}_x)_{1-y}\text{S}$  is taken as abscissa and  $T_t$  as ordinate. The short vertical lines indicate the width of thermal hysteresis. The upper end of vertical lines corresponds to  $T_t$  in heating run, and the lower end  $T_t$  in cooling run. The inset shows the aging effects on  $T_t(F)$  ( $T_t$  in the forward direction) for  $(\text{Ni}_{0.8}\text{Fe}_{0.2})_{1-y}\text{S}$ . The vertical lines indicate the increase of  $T_t(F)$  for various "1-y" compositions. Aging temperature is 290 K. Detail is described in the text.

**Phase Transition.** Transition temperatures were determined mainly by the DSC method. The method of determination of  $T_t$  is shown in Fig. 3(b).  $T_t$  is very sensitive to thermal history. Results of unaged specimens are as follows. Variation of  $T_t$  with Fe contents is given in Fig. 2, where  $x$  in  $(\text{Ni}_{1-x}\text{Fe}_x)_{1-y}\text{S}$  is taken as abscissa and  $T_t$  as ordinate.  $T_t$  was measured on heating-cooling cycles on specimens immediately after quenching from 800 °C. Endothermic and exothermic peaks were observed for heating and cooling, respectively. The value of  $T_t$  remained unchanged with heating-cooling rate. When "1-y" is fixed,  $T_t$  increases smoothly with increasing  $x$ . All curves of constant "1-y" seem to cross at  $x=0.30$  (ca. 360 K). At  $x=0.30$ , DSC peaks are somewhat broadened after the first heating run, and for  $x>0.30$ , no DSC peaks could be detected in any "1-y" composi-

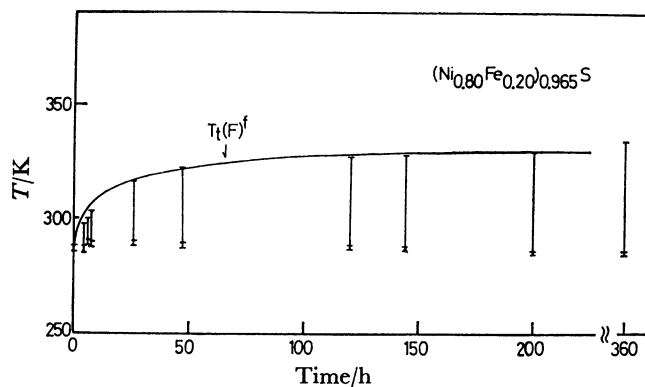


Fig. 3(a).  $T_t$  as a function of aging time for  $(\text{Ni}_{0.8}\text{Fe}_{0.2})_{0.985}\text{S}$ . Aging temperature is 290 K. The time elapsed from immediately after quenching is taken as abscissa. The upper end of vertical lines corresponds to  $T_t$  in the forward direction in the first heating run. Two horizontal lines in the lower end of vertical lines show the hysteresis width in the subsequent heating-cooling runs.

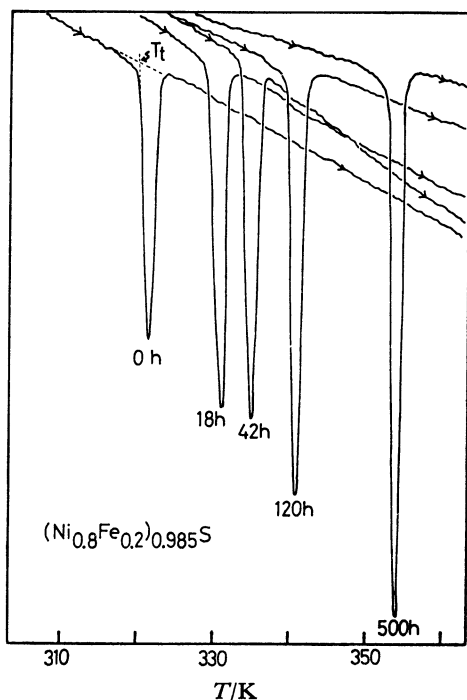


Fig. 3(b). The variation of DSC curves in the first heating runs with time elapsed for  $(\text{Ni}_{0.8}\text{Fe}_{0.2})_{0.985}\text{S}$ . Aging temperature is 290 K. Transition is endothermic.

tion. The short vertical lines in Fig. 2 indicate the width of thermal hysteresis observed in heating-cooling runs. The width of thermal hysteresis is within several degrees, and seems to be independent of composition. Hereafter,  $T_t$  in the heating run (forward direction) is referred to as  $T_t(\text{F})$ , and  $T_t$  in the cooling run (reverse direction)  $T_t(\text{R})$ .

The results on aged specimens are as follows. The forward transformation shows an anomalous thermal hysteresis in aged specimens. When samples are aged at temperatures below  $T_t(\text{R})$ ,  $T_t(\text{F})$  gradually increases with the lapse of time and after sufficiently long time

(about 20 days), reaches the final  $T_t(\text{F})$  (the final  $T_t(\text{F})$  is referred to as  $T_t(\text{F})^f$ ), which is about 50 degrees higher than the initial  $T_t(\text{F})$  (the initial  $T_t(\text{F})$  is referred to as  $T_t(\text{F})^i$ ).  $T_t$  as a function of the time elapsed in the case of  $(\text{Ni}_{0.8}\text{Fe}_{0.2})_{0.985}\text{S}$  aged at 290 K is shown in Fig. 3(a). The vertical lines show the width of increase of  $T_t(\text{F})$ . Endothermic DSC peaks of  $(\text{Ni}_{0.8}\text{Fe}_{0.2})_{0.985}\text{S}$  in the first heating run are shown for various aging times, the aging temperature being 290 K (Fig. 3(b)). No evidence of extra peaks can be detected throughout aging. The shape of DSC peaks is very sharp at all aging times, the height of peaks increasing with increasing  $T_t(\text{F})$ . The inset in Fig. 2 illustrates the “ $1-y$ ” dependence of the width of increase of  $T_t(\text{F})$  for  $x=0.20$ . The upper end of the vertical line corresponds to  $T_t(\text{F})^f$ . The width of increase of  $T_t(\text{F})$  seems to decrease with increasing “ $1-y$ ”. The tendency, however, is somewhat ambiguous since the width of increase of  $T_t(\text{F})$  is sensitive to experimental conditions.  $x$  dependence of  $T_t(\text{F})$  is shown in Fig. 4 for

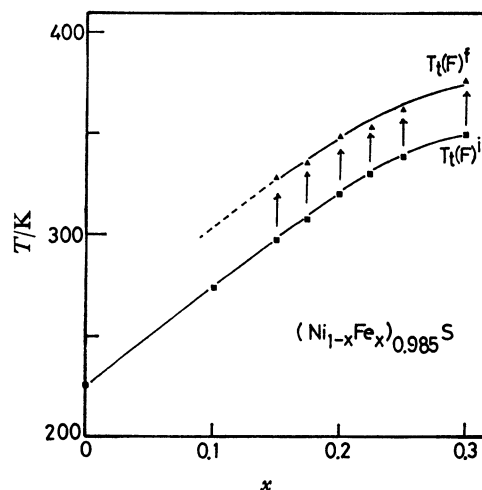


Fig. 4.  $x$  dependence of  $T_t(\text{F})$  ( $T_t$  in the forward direction) for  $(\text{Ni}_{1-x}\text{Fe}_x)_{0.985}\text{S}$ . Aging temperature is 290 K. Arrows show the increase of  $T_t(\text{F})$  by aging. The closed triangles show the final  $T_t(\text{F})$  ( $T_t(\text{F})^f$ ). The closed squares show the initial  $T_t(\text{F})$  ( $T_t(\text{F})^i$ ).

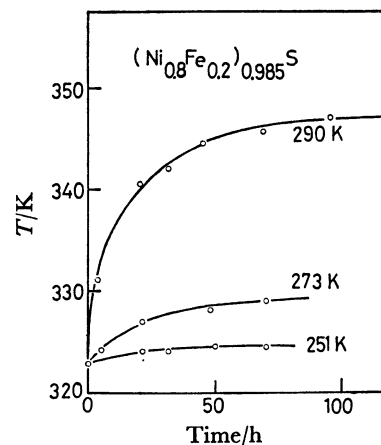


Fig. 5. Aging time dependence of transition temperatures in the first heating run of  $(\text{Ni}_{0.8}\text{Fe}_{0.2})_{0.985}\text{S}$  for various aging temperatures (290, 273, and 251 K).

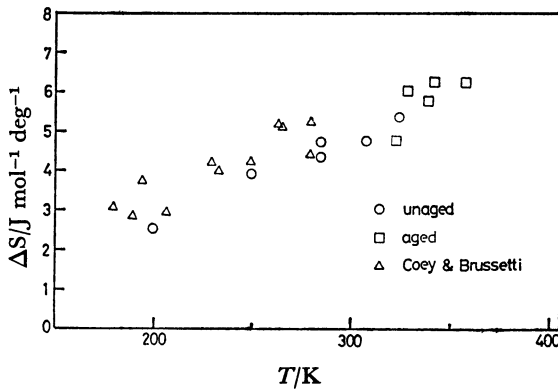


Fig. 6. Entropy change at  $T_t$  ( $\Delta S$ ) as a function of  $T_t$  for  $(\text{Ni}_{1-x}\text{Fe}_x)_{1-y}\text{S}$  system. Open circles show  $\Delta S$  for unaged specimens. Open square is  $\Delta S$  for sufficiently aged specimens. Open triangles are those obtained by Coey and Brussetti.<sup>21)</sup>

$(\text{Ni}_{1-x}\text{Fe}_x)_{0.985}\text{S}$  which was aged at 290 K. The lower curve shows the  $x$  dependence of  $T_t(\text{F})^i$  and the upper curve that of  $T_t(\text{F})^f$ . The width of increase of  $T_t(\text{F})$  seems to be independent of  $x$ . In specimens of  $x \leq 0.10$ , the increase could not be observed since  $T_t(\text{R})$  is lower than 290 K. Figure 5 shows the variation of  $T_t(\text{F})$  with aging temperature for  $(\text{Ni}_{0.8}\text{Fe}_{0.2})_{0.985}\text{S}$ . Samples were aged at 290 K, 273 K (in ice water) and 251 K (in a mixture of ice, water, and NaCl). Increase in rate is more rapid at the higher aging temperatures. We tried to carry out aging at temperature immediately below  $T_t(\text{F})^f$  after aging for a sufficiently long time at 290 K. We could observe no more increase of  $T_t(\text{F})$ . Increase of  $T_t(\text{F})$ , however, was also observed in the case of aging at slightly higher temperatures (less than 5 degrees higher) than  $T_t(\text{F})^i$ . Figure 6 shows the variation of entropy change ( $\Delta S$ ) at the transition with  $T_t$ .  $\Delta S$  was determined from the endothermic peaks. Open circles show the entropy changes of unaged specimens, and open squares those of specimens aged for a sufficiently long time. We see that entropy change at the transition increases almost linearly with increasing  $T_t$ . We can recognize no significant difference of entropy change between unaged and aged specimens. For example,  $\Delta S$  of  $(\text{Ni}_{0.8}\text{Fe}_{0.2})_{0.985}\text{S}$  is 4.26 and 6.01  $\text{J mol}^{-1} \text{deg}^{-1}$  for unaged and aged specimens, respectively: both values fit the curve in Fig. 6. Our results are almost the same as those of Coey and Brussetti<sup>21)</sup> shown by open triangles.

The increase of  $T_t(\text{F})$  was observed only in the first heating run. When aged samples are once passed through  $T_t(\text{F})$  ( $>T_t(\text{F})^i$ ), transition temperatures in the subsequent cooling and heating runs return to the initial  $T_t(\text{R})$  and  $T_t(\text{F})$  (Fig. 7(a)). When the samples are again aged at temperatures below  $T_t(\text{R})$ ,  $T_t(\text{F})$  increases asymptotically approaching  $T_t(\text{F})^f$ , as in the previous aging process.

Aging effects on other physical properties were examined. X-ray powder diffraction measurements were performed on specimens aged for a sufficiently long time. No extra diffraction peak or shift of diffraction peaks was found. The temperature dependence of lattice spacings of  $(\text{Ni}_{0.8}\text{Fe}_{0.2})_{0.985}\text{S}$  aged at 290 K

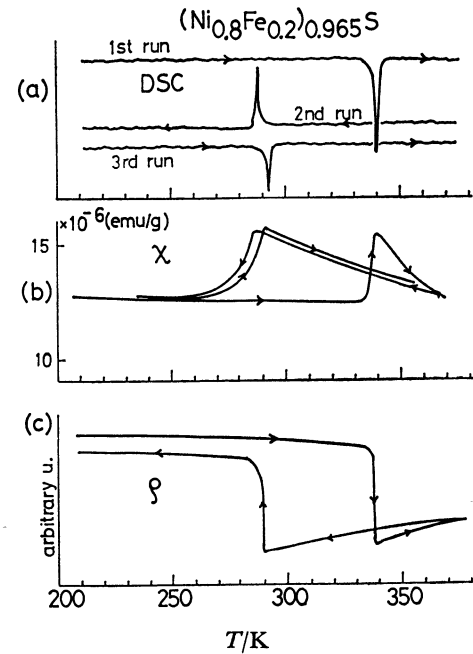


Fig. 7. Typical behaviors of the transition in the first heating run and subsequent cooling-heating runs for  $(\text{Ni}_{0.8}\text{Fe}_{0.2})_{0.985}\text{S}$  aged for a long time at 290 K. (a): DSC curves, (b): magnetic susceptibility, (c): electrical resistivity.

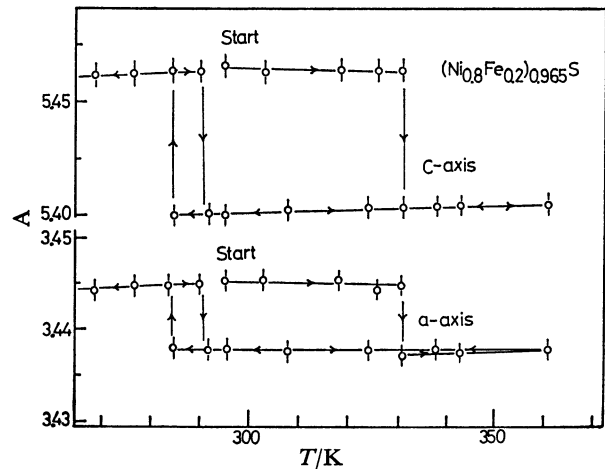


Fig. 8. Lattice spacings of  $(\text{Ni}_{0.8}\text{Fe}_{0.2})_{0.985}\text{S}$  as a function of temperature. X-Ray measurements were done firstly on heating run for a sufficiently long time aged specimens, and subsequently on cooling run. Procedure of measurements is shown by arrows.

for sufficiently long time is shown in Fig. 8. The order of X-ray diffraction measurements is indicated by arrows. Both a- and c-parameters decrease slightly with temperature in the first heating run. Abrupt shrinkage was observed at  $T_t(\text{F})^f$ , and abrupt expansion at  $T_t(\text{R})$  in the cooling run. In the second heating run, the transition was observed at  $T_t(\text{F})^i$ . The results are in line with those of DSC measurements. Typical electrical resistivity ( $\rho$ ) as a function of temperature is shown in Fig. 7(c) for  $(\text{Ni}_{0.8}\text{Fe}_{0.2})_{0.985}\text{S}$  aged for a long time. In Fig. 9, the electrical resistivity ( $\rho$ )

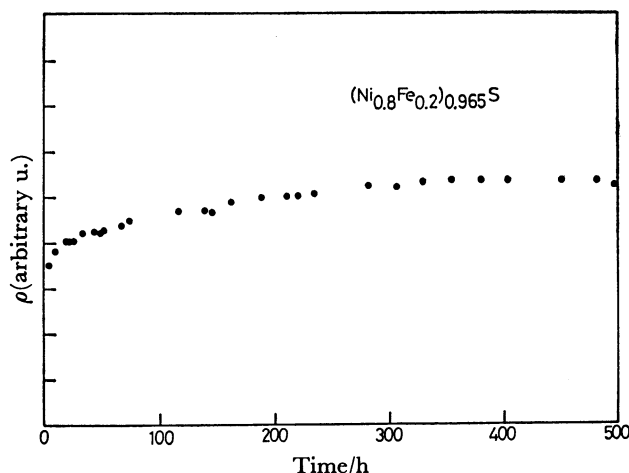


Fig. 9. Aging time dependence of electrical resistivity of  $(\text{Ni}_{0.8}\text{Fe}_{0.2})_{0.985}\text{S}$ . Aging temperature is 290 K.

at 290 K is plotted against the lapse of time for  $(\text{Ni}_{0.8}\text{Fe}_{0.2})_{0.985}\text{S}$  which was quenched from 800 °C. Since  $T_t(\text{F})^i$  is slightly above 290 K,  $T_t(\text{F})$  increases with time elapsed. Resistivity increases with time elapsed and seems to be saturated after aging for *ca.* 400 h. Magnetic susceptibility ( $\chi$ ) of  $(\text{Ni}_{1-x}\text{Fe}_x)_{0.985}\text{S}$  ( $x \leq 0.30$ ) aged for sufficiently long time is given in Fig. 10 as a function of temperature. Heating and cooling cycles are shown by arrows. Typical behavior of  $\chi$  is shown in Fig. 7(b) for  $(\text{Ni}_{0.8}\text{Fe}_{0.2})_{0.985}\text{S}$  aged for a long time. The kinks in  $\chi$  curves correspond to the transition. The difference of  $\chi$  between aged and unaged samples is very small except for near transition. There is a broad maximum in  $\chi$  curves in samples of  $x \geq 0.250$  at about 140 K, while  $\chi$  of the other samples is almost constant with temperature. The results of Mössbauer measurements are shown in Fig. 11. Measurements were carried out for both aged (for 20 d) and unaged specimens of  $(\text{Ni}_{0.8}\text{Fe}_{0.2})_{0.985}\text{S}$ . An absorption spectrum with quadrupole splitting was observed at 373 K

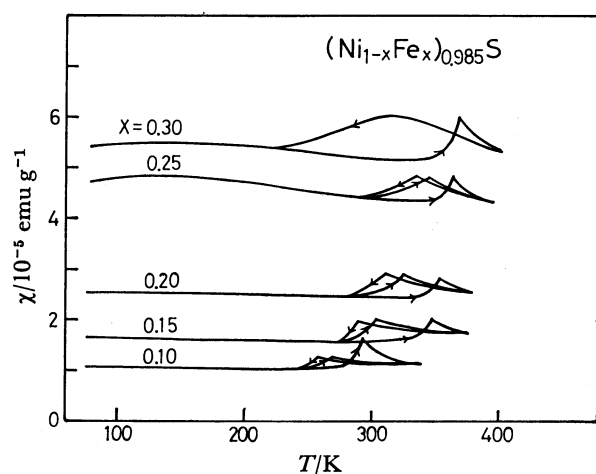


Fig. 10. Magnetic susceptibility of sufficiently long time aged  $(\text{Ni}_{1-x}\text{Fe}_x)_{0.985}\text{S}$  ( $x \leq 0.30$ ) as a function of temperature. Heating-cooling cycles are shown by arrows.

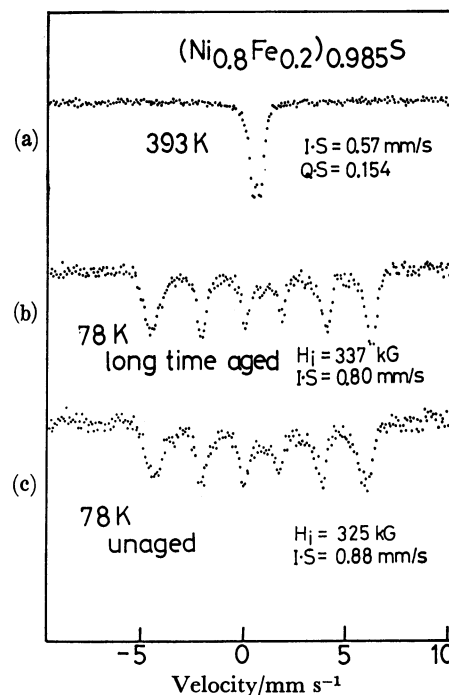


Fig. 11. Mössbauer spectra for  $(\text{Ni}_{0.8}\text{Fe}_{0.2})_{0.985}\text{S}$ .

(a): Spectra at 393 K (above  $T_t(\text{F})^i$ ), (b): spectra at 78 K for a long time aged specimen, (c) spectra at 78 K for unaged specimen.

(Fig. 11(a)), the isomer shift and quadrupole splitting being 0.57 and 0.154 mm/s, respectively. Magnetic sextets were observed at 78 K. Figures 11(b) and (c) show the results obtained at 78 K for  $(\text{Ni}_{0.8}\text{Fe}_{0.2})_{0.985}\text{S}$  aged for a long time and unaged, respectively. Internal magnetic field is  $2.68 \times 10^7$  and  $2.59 \times 10^7 \text{ A m}^{-1}$  for aged and unaged specimen, respectively. Isomer shift is 0.80 and 0.88 mm/s for aged and unaged specimen, respectively.

The results of anomalous thermal hysteresis are summarized as follows.

a)  $T_t(\text{F})$  increases with time, when the specimens are aged at temperature below  $T_t(\text{R})$ .  $T_t(\text{F})^i$  is *ca.* 50 degrees higher than  $T_t(\text{F})^i$ .  $T_t(\text{F})$  is unchanged when specimens are aged at temperatures above  $T_t(\text{F})$ .  $T_t(\text{R})$  is not affected by heat treatment.

b) When aged specimens are once passed through  $T_t(\text{F})$  ( $> T_t(\text{F})^i$ ),  $T_t(\text{F})$  in the subsequent heating runs return to  $T_t(\text{F})^i$ . When samples are again aged at temperatures below  $T_t(\text{R})$ , the same aging effects are also observed.

c) Two phase mixture of the initial and the final state is not observed in the course of aging in both DSC curves and X-ray powder diffraction patterns. No new phase was observed during the course of aging.

d) Increase in the rate of  $T_t(\text{F})$  increases with rise in aging temperature.

e) The width of increase of  $T_t(\text{F})$  seems to be almost independent of  $x$  composition.

f) The nature of phase transition, *i.e.* metal-semiconductor transition accompanied by magnetic change, is essentially unchanged by aging treatment. Physical properties of both aged and unaged specimens are

compared as follows.

- 1) No crystallographical difference is found in X-ray diffraction patterns.
- 2) Electrical resistivity of aged specimens is higher than that of unaged one.
- 3) Difference of magnetic susceptibility is very small.
- 4) Internal magnetic field of aged specimen is higher than that of aged one.

### Discussion

In the course of studies on the phase transition of  $(\text{Ni}_{1-x}\text{Fe}_x)_{1-y}\text{S}$  system, we found anomalous aging effects on the transition temperature. First let us consider the phase relation of this system. Misra and Fleet<sup>26)</sup> have reported the monosulfide solid solution in the temperature range 230–600 °C. They found extra peaks such as super lines in powder patterns of all of monosulfide-bearing products. However, we found no extra peak in X-ray diffraction patterns, confirming the distinct region of solid solution of this system. Solid solution was also confirmed by DSC measurements which show smooth increase of the transition temperature with Fe contents up to 30 at. %. Barthelemy *et al.*<sup>19)</sup> found two phases in  $\text{Ni}_{1-x}\text{Fe}_x\text{S}$  with small amount of Fe at 550 °C, one with  $0 \leq x \leq 0.05$ , the other with  $0.10 \leq x \leq 0.20$  and a mixture of two phases with  $0.05 < x < 0.10$ . c-parameter of the second phase is greater than that of the first one. This can be explained by our results of aging effects.  $T_t$  in the composition range of  $0.05 < x < 0.10$  lies near room temperature. Thus, in the range  $0 \leq x \leq 0.05$ , X-ray diffraction patterns at room temperature show a pattern of the H-phase; in the range  $0.10 \leq x \leq 0.20$  they show one of the L-phase which has a greater c-parameter than the H-phase. Two phase mixture in the region  $0.05 < x < 0.10$  can be explained by the following results. In specimens which have  $T_t$  slightly below room temperature,  $T_t$  gradually increases with the lapse of time at room temperature. X-Ray diffraction patterns at room temperature show the two phase mixture of the H- and L-phases, both phases having the NiAs type structure while lattice spacings differ from each other. Two phase mixture has been observed for 48 h in X-ray charts; this feature is remarkable especially in (102) reflection. No lattice modification was found in the  $(\text{Ni}_{1-x}\text{Fe}_x)_{1-y}\text{S}$  system.

The phase transition of this system is accompanied by the drastic changes of electrical and magnetic properties, this being metal-semiconductor transition similar to that of pure NiS.  $(\text{Ni}_{1-x}\text{Fe}_x)_{1-y}\text{S}$  with Ni-rich composition has substantially the same characteristics of phase transition as that of pure NiS.

Let us consider the aging effects on the phase transition. It is important to examine whether this is characteristic of only Fe substituted  $\text{Ni}_{1-y}\text{S}$ . Trahan and Goodrich<sup>22)</sup> found in their calorimetric measurements that it takes a long time for stoichiometric NiS to attain equilibrium near the transition, exhibiting a considerable hysteresis.  $T_t$  was observed to be 276 K in heating run, and 269 K in cooling run, while in cooling run the samples supercooled approximately by 2.5 K. All

previous publications except that of Trahan and Goodrich reported that  $T_t$  of NiS lies in the neighbourhood of 265 K. The anomalous high transition temperature in heating runs of Trahan and Goodrich is presumably due to the aging effects. For the sake of confirmation we performed DSC measurements for undoped NiS. We observed the increase of  $T_t(\text{F})$ :  $T_t(\text{F})$  increases by about 1 degree by annealing at 250 K for 24 h, in line with the data of Fig. 5. Thus the increase of  $T_t(\text{F})$  by aging is considered to be characteristic phenomenon in NiS as well as in  $(\text{Ni}_{1-x}\text{Fe}_x)_{1-y}\text{S}$ .

The phenomenon can be regarded as thermal hysteresis, a common feature of the first order transition. In the reversible transformation of the first order, the hysteresis width is closely related to the volume change at the transition,  $\Delta V$ .<sup>28,29)</sup> For example, for the transition of  $\text{NH}_4\text{Cl}$  ( $\text{P}_{\text{m}3\text{m}} \rightarrow \text{F}_{\text{m}3\text{m}}$ ) the width of hysteresis is 35 K, and  $\Delta V + 7.14 \text{ cm}^3/\text{mol}$ ; for  $\text{CsCl}$  ( $\text{P}_{\text{m}3\text{m}} \rightarrow \text{F}_{\text{m}3\text{m}}$ ) hysteresis width is 33 K,  $\Delta V + 10.28 \text{ cm}^3/\text{mol}$ . In the case of  $(\text{Ni}_{1-x}\text{Fe}_x)_{1-y}\text{S}$ , the reversible thermal hysteresis is observed in unaged specimens, where the hysteresis width is several degrees. This seems to be reasonable since  $\Delta V$  is relatively small, *ca.*  $-0.3 \text{ cm}^3/\text{mol}$ . The increase of  $T_t(\text{F})$  by aging, as high as 50 degrees, seems to be enormously large.

Gradual increase of  $T_t(\text{F})$  with aging indicates that the initial unaged state is in thermally non-equilibrium, passing gradually into equilibrium. This has been reported, *e.g.* anatase-rutile or brookite-rutile in  $\text{TiO}_2$ ,<sup>30)</sup> or hexagonal-tetragonal transformation in  $\text{GeO}_2$ .<sup>31)</sup> The transformation is a function of time and temperature. In the transient state from metastable to stable one, two phases usually coexist. Transformation kinetics has been investigated by using the Avrami equation. The present case differs a great deal from above cases. DSC measurements show continuous shift of  $T_t(\text{F})$ , but X-ray diffraction measurements show no two phase mixture. Thus, the present case can not

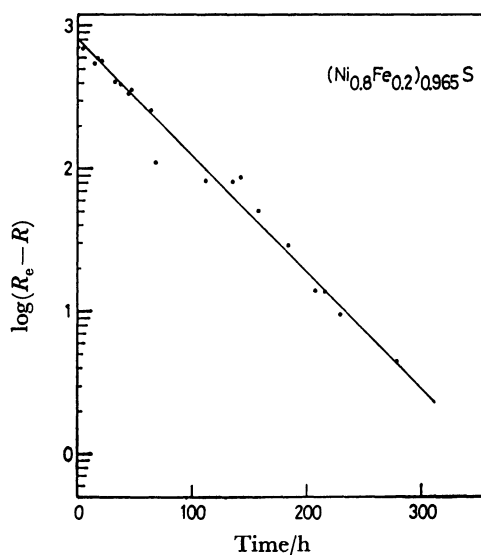


Fig. 12. The logarithm of  $(R_e - R)$  as a function of elapsed time.  $(R_e - R)$  is the difference between the resistivity at  $t = \infty$  and time  $t$ .

be interpreted in a similar manner to the above substance.

As shown in Fig. 9, the electrical resistivity ( $\rho$ ) increases very gradually with elapsed time if samples are aged at 290 K (below  $T_t(R)$ ). After a sufficiently long time,  $\rho$  attained the value of thermal equilibrium state,  $R_e$ . In Fig. 12, the logarithm of the difference between the resistivity at time  $t=\infty$  and time  $t$ , ( $R_e - R$ ) is plotted against  $t$  (data are the same as in Fig. 9). For an exponential change the graph should be a straight line, and this is the case. Thus, it is presumed that the time dependence of  $\rho$  has the form

$$R_e - R = Ae^{-t/\tau},$$

where  $A$  is a constant and  $\tau$  the relaxation time. From the slope, we estimated  $\tau$  to be 118 h. A similar treatment was performed by Trahan and Goodrich,<sup>22)</sup> who measured the electrical resistivity near the transition temperature of stoichiometric NiS, and estimated  $\tau$  to be 48 h. They did not, however, specify the aging temperature. From analogy with the present case, we suppose their measurements were taken at temperature below  $T_t(R)$ . Thus, we can conclude that the aging effect is the relaxation process from thermally non-equilibrium state to equilibrium one.

Generally, phase transition is described in terms of nucleation and growth. At the start of transition, the nuclei of a new phase are first formed in the parent phase, followed by development of the new phase. If specific volumes differ from each other, the product phase in the parent phase produces strain. If the parent phase is not sufficiently soft, the elastic strain energy might be stored in the crystal. The interfacial energy formed between the product and the parent phase should also be considered. Ubbelohde<sup>32)</sup> suggested that extra terms for the strain energy and the interfacial energy should be added to the usual independent variables that determine the free-energy; the strain energy is a main factor controlling thermal hysteresis.

We should consider the following characteristics of the transition. The transition is accompanied by drastic volume expansion with fall in temperature (about 2.0%). The material becomes brittle below  $T_t$ ; i.e. specimens cracked through transition with lowering temperature. The mechanism of phase transition differs for the case of the forward and reverse directions. In the forward direction (a), the relatively soft phase grows in the brittle phase associated with volume contraction, while in the reverse direction (b) a brittle phase grows in soft matrix associated with volume expansion. In (a) the product phase is strained under tension, and in (b) it is strained under compression. The large difference in the sensitivity of the transition temperature between (a) and (b) may be due to such different transition mechanism. Since the L-phase is brittle, it has a larger contribution to the strain energy than the H-phase. Thus, (a) would be more sensitive to the thermal treatments than (b).

Considering the L-phase which is in a state immediately after reverse transition (non-equilibrium state), excess energy such as strain energy would be expected to be stored in the crystal. Such a state would

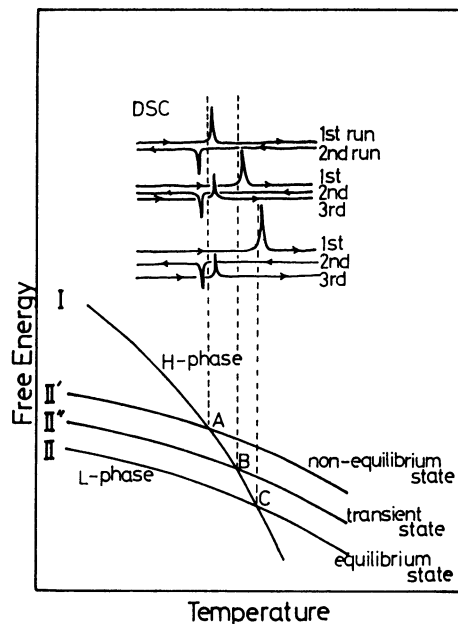


Fig. 13. Tentative Gibbs free-energy diagram for  $(\text{Ni}_{1-x}\text{Fe}_x)_{1-y}\text{S}$  system. Curve I, II, II', and II'' are Gibbs free-energy curves of the H-phase, equilibrium state of L-phase, non-equilibrium state of L-phase and the transient state from non-equilibrium to equilibrium state of L-phase, respectively. Free-energy curve of nonequilibrium state is in a higher energy state than the equilibrium state due to the stored strain energy in the L-phase. Curve I is assumed to be invariant to thermal treatments. The upper side of the figure indicates DSC curves corresponding to each state.

be in a higher energy state than the equilibrium state stabilized by aging for long time below  $T_t(R)$ . Thus, free energy-temperature curve for the non-equilibrium state is expected to lie slightly above that of the equilibrium one. Such a relation is schematically illustrated in Fig. 13, where curves I, II, II', and II'' are Gibbs free-energy curves, corresponding to the H-phase, the equilibrium state of L-phase, the nonequilibrium state of L-phase and the transient state from non-equilibrium to equilibrium state of L-phase, respectively. Curve I is assumed to be independent of thermal history of the specimens. Curve II', II'', and II intersect with curve I at points A, B, and C, respectively. DSC curves are shown for each state. Relaxation phenomenon would be considered to be the process where the stored strain energy is relieved by aging, corresponding to the lowering in free energy curve from II' to II, accompanied by the increase of transition temperature.

The relaxation phenomenon would be also considered as an order-disorder process, where non-equilibrium disordered state is transformed to the equilibrium ordered state with aging. The disordered state would be expected to have higher energy than the ordered one. In Fig. 13, the disordered state corresponds to curve II', and the ordered state curve II. The order-disorder transition is considered to occur at the same temperature as  $T_t(F)$ . If this is not the case, aging effect should be observed also in the H-phase. This mechanism,

however, does not seem to be applicable to the present case. If the ordering is due to metal vacancies, superlines due to ordering should be observed in X-ray charts. This could not be confirmed. If the ordering process occurred between Ni and Fe atoms, no aging effects should be observed in pure NiS. According to Trahan and Goodrich,<sup>22)</sup> and our present measurements, aging effects were observed also in NiS. The difference of entropy change at  $T_t$  between aged and unaged state could not be detected by DSC measurements.

So far, aging effects similar to the present case have been observed in a few materials. Murray and Allison<sup>33)</sup> observed the aging effects in  $\text{ZrO}_2$ , where the tetragonal to monoclinic phase transition (reverse transition) is slightly affected by heat treatments; *i.e.* the transition temperature of the reverse direction is drastically raised by either heating-cooling cycles through the transition or aging at tetragonal phase (above the transition temperature). They interpreted this phenomenon as the ordering process in the tetragonal phase. On the other hand, Maiti *et al.*<sup>34)</sup> attributed this to the superplastic nature of the tetragonal phase. Another example was reported by Murakami *et al.*,<sup>35)</sup> who found a very similar phenomenon to the present case in Au-Cu-Zn alloys. Martensite reverse transition temperature of  $\text{Au}_{26}\text{Cu}_{30}\text{Zn}_{44}$  alloy increases by about 20 K, when it is aged at 290 K (below the transition temperature). They assumed that the aging effect is due to the stabilization and pinning of the martensite plate boundaries, which give rise to an increase in the driving force for the transition.

In conclusion, we have observed a new type of thermal hysteresis in  $(\text{Ni}_{1-x}\text{Fe}_x)_{1-y}\text{S}$  system. It is considered to be a relaxation process where the strain energy stored in the L-phase is relieved by aging.

The author wish to express their sincere thanks to Prof. T. Takada and Dr. T. Shinjo for enabling them to carry out the Mössbauer measurements.

## References

- 1) M. Laffitte, *Bull. Soc. Chim. Fr.*, **1959**, 1211.
- 2) J. T. Sparks and T. Komoto, *J. Appl. Phys.*, **34**, 1191 (1963).
- 3) J. T. Sparks and T. Komoto, *Phys. Lett. A*, **25**, 398 (1968).
- 4) J. T. Sparks and T. Komoto, *Rev. Mod. Phys.*, **40**, 752 (1968).
- 5) J. Trahan, R. G. Goodrich, and S. F. Watkins, *Phys. Rev. B*, **2**, 2859 (1970).
- 6) D. B. McWhan, M. Marezio, J. P. Remeika, and P. D. Dernier, *Phys. Rev. B*, **5**, 2552 (1972).
- 7) T. Ohtani, K. Kosuge, and S. Kachi, *J. Phys. Soc. Jpn.*, **28**, 1558 (1970).
- 8) T. Ohtani, K. Kosuge, and S. Kachi, *J. Phys. Soc. Jpn.*, **29**, 521 (1970).
- 9) T. Ohtani, *J. Phys. Soc. Jpn.*, **37**, 701 (1974).
- 10) M. G. Townsend, R. Tremblay, J. L. Horwood, and L. B. Ripley, *J. Phys. C*, **4**, 598 (1971).
- 11) J. L. Horwood, L. G. Ripley, M. G. Townsend, and R. J. Tremblay, *J. Appl. Phys.*, **42**, 1476 (1971).
- 12) E. Barthelemy, O. Gorochoy, and M. McKinzie, *Mat. Res. Bull.*, **8**, 1401 (1973).
- 13) J. M. D. Coey, R. Brussetti, A. Kallel, J. Schweizer, and H. Fuess, *Phys. Rev. Lett.*, **32**, 1257 (1974).
- 14) R. Brussetti, Thesis, Grenoble University, 1978.
- 15) S. Anzai and K. Ozawa, *J. Phys. Soc. Jpn.*, **24**, 271 (1968).
- 16) S. Anzai and K. Ozawa, *J. Appl. Phys.*, **48**, 2139 (1977).
- 17) T. Ohtani, K. Kosuge, and S. Kachi, *Phys. Status Solidi B*, **66**, 765 (1974).
- 18) T. Sawa and S. Anzai, *J. Appl. Phys.*, **49**, 5612 (1978).
- 19) E. Barthelemy, C. Chavant, G. Collin, and O. Gorochoy, *J. Phys. (Paris), Colloq.*, **37**, C4-17 (1976).
- 20) R. F. Koehler, Jr., R. S. Feigelson, H. W. Swarts, and R. L. White, *J. Appl. Phys.*, **43**, 3127 (1972).
- 21) J. M. D. Coey and R. Brussetti, *Phys. Rev. B*, **11**, 671 (1975).
- 22) J. Trahan and R. G. Goodrich, *Phys. Rev. B*, **6**, 199 (1972).
- 23) J. M. D. Coey, H. Roux-Buisson, and R. Brussetti, *J. Phys. (Paris), Colloq.*, **37**, C4-1 (1976).
- 24) S. Kachi, K. Kosuge, and H. Okinaka, *J. Solid State Chem.*, **6**, 258 (1973).
- 25) R. M. White and N. F. Mott, *Philos. Mag.*, **24**, 845 (1972).
- 26) K. C. Misra and M. E. Fleet, *Mat. Res. Bull.*, **8**, 669 (1973).
- 27) T. Ohtani, K. Kosuge, and S. Kachi, *Phys. Status Solidi B*, **96**, K69 (1979).
- 28) D. C. Thomas and L. A. K. Staveley, *J. Chem. Soc.*, **1420**, 2572 (1951).
- 29) K. J. Rao and C. N. R. Rao, *J. Mater. Sci.*, **1**, 238 (1966).
- 30) A. W. Czanderna, C. N. R. Rao, and J. M. Honig, *Trans. Faraday Soc.*, **54**, 1069 (1958).
- 31) Y. Kotera and M. Yonemura, *Trans. Faraday Soc.*, **59**, 147 (1963).
- 32) A. R. Ubbelohde, *Quart. Rev. Chem. Soc. (London)*, **11**, 246 (1957).
- 33) P. Murray and E. B. Allison, *Trans. Brit. Ceram. Soc.*, **53**, 335 (1954).
- 34) H. S. Maiti, K. V. G. K. Gokhale, and E. C. Subbarao, *J. Am. Ceram. Soc.*, **55**, 317 (1972).
- 35) Y. Murakami, S. C. Singh, and L. Delaey, *Scripta Met.*, **12**, 1095 (1978).